© 2022. Published by The Company of Biologists Ltd | Development (2022) 149, dev200282. doi:10.1242/dev.200282

STEM CELLS AND REGENERATION

RESEARCH ARTICLE

Newt *Hoxa13* has an essential and predominant role in digit formation during development and regeneration

Takashi Takeuchi[1,§,¶], Haruka Matsubara[1,§], Fumina Minamitani[1], Yukio Satoh[1], Sayo Tozawa[1], Tomoki Moriyama[1], Kohei Maruyama[1], Ken-ichi T. Suzuki[2], Shuji Shigenobu[2], Takeshi Inoue[3,*], Koji Tamura[4], Kiyokazu Agata[2,3] and Toshinori Hayashi[1,5,‡]

ABSTRACT

The 5′Hox genes play crucial roles in limb development and specify regions in the proximal-distal axis of limbs. However, there is no direct genetic evidence that Hox genes are essential for limb development in non-mammalian tetrapods or for limb regeneration. Here, we produced single to quadruple Hox13 paralog mutants using the CRISPR/Cas9 system in newts (*Pleurodeles waltl*), which have strong regenerative capacities, and also produced germline mutants. We show that Hox13 genes are essential for digit formation in development, as in mice. In addition, *Hoxa13* has a predominant role in digit formation, unlike in mice. The predominance is probably due to the restricted expression pattern of *Hoxd13* in limb buds and the strong dependence of *Hoxd13* expression on *Hoxa13*. Finally, we demonstrate that Hox13 genes are also necessary for digit formation in limb regeneration. Our findings reveal that the general function of Hox13 genes is conserved between limb development and regeneration, and across taxa. The predominance of *Hoxa13* function both in newt limbs and fish fins, but not in mouse limbs, suggests a potential contribution of *Hoxa13* function in fin-to-limb transition.

KEY WORDS: Hox13, Digit formation, Limb development, Limb regeneration, Urodele amphibians, Fin-to-limb transition

INTRODUCTION

The 5′Hox genes play crucial roles in pattern formation and growth along the proximal-distal and anterior-posterior axes during limb development (for a review, see Zákány and Duboule, 2007). The expression patterns and phenotypes of spontaneous and gene knockout mutants support a model in which Hox9/10, Hox11 and Hox12/13 paralogs specify the identity of the stylopod, zeugopod and autopod, respectively, during limb development (Davis et al., 1995; Fromental-Ramain et al., 1996a,b; Wellik and Capecchi, 2003; Zákány and Duboule, 2007). In the case of the autopod, *Hoxa13* and *Hoxd13* presumably specify the distal autopod, because double-mutant mice lacking *Hoxa13* and *Hoxd13* lose all their digits and metacarpal/tarsal bones (Fromental-Ramain et al., 1996b). These genes also regulate the development of the autopod in human limbs, because disorders of digit formation, such as hypodactyly, have been linked to human mutations in *HOXA13* and *HOXD13* (for a review, see Lappin et al., 2006).

Unlike in mammals, there is no direct genetic evidence that the 5′Hox genes are essential for limb development in non-mammalian tetrapod vertebrates. Instead of genetic studies, the expression patterns of 5′Hox genes have been examined during limb development in various non-mammalian tetrapods, such as chickens, frogs and axolotls. Although there are differences between species, these overall expression patterns are similar to those of mice (Bickelmann et al., 2018; Gardiner et al., 1995; Satoh et al., 2006; Torok et al., 1998; Wagner et al., 1999; Woltering et al., 2019), suggesting that the basic functions of 5′Hox genes are conserved in tetrapod limb development. However, their conservation is not conclusive because no functional analyses, such as by using genetics, have been performed. In addition, it is still unknown what functions of the 5′Hox genes are specific for which species and how their specificity is related to the distinct morphology and functions of limbs in various taxa.

In addition to limb development in non-mammalian tetrapods, it is still unknown whether Hox functions are essential for limb regeneration. Furthermore, if they are essential, it is not known whether Hox genes also have regeneration-specific functions. These issues are strongly related to how similar regeneration is to development, and to what is specific about regeneration. To investigate the roles of Hox genes in limb regeneration and their similarity or specificity, Hox expression patterns during limb regeneration have been examined in axolotls. Their expression in blastemas is similar to that in developing limb buds, except for the simultaneous expression of *Hoxa13* and *Hoxa9* within 24 h after amputation (Gardiner et al., 1995; Torok et al., 1998). However, the early expression pattern was not supported by analysis using antibodies against Hox proteins (Roensch et al., 2013). In any case, Hox genes are expected to have crucial functions in limb regeneration, and regeneration-specific functions have not been excluded.

One major reason why genetic analyses have not been performed in non-mammalian tetrapods has been the lack of reverse genetic techniques other than in rodents. In particular, gene disruption had not been achieved in animals that can regenerate their limbs. However, genome editing using CRISPR/Cas9 has been established as an efficient tool for gene disruption in many species and has enabled functional studies in many organisms. In addition, several

[1]Division of Developmental Biology, School of Life Sciences, Faculty of Medicine, Tottori University, 86 Nishi-cho, Yonago, Tottori 683-8503, Japan. [2]Laboratory of Regeneration Biology, National Institute for Basic Biology, Nishigonaka 38, Myodaiji, Okazaki, Aichi 444-8585, Japan. [3]Department of Life Science, Faculty of Science, Gakushuin University, Toyoshima-Ku, Tokyo 171-8588, Japan. [4]Department of Developmental Biology and Neurosciences, Graduate School of Life Sciences, Tohoku University, Aoba-ku, Sendai, 980-8578, Japan. [5]Program of Biomedical Science, Graduate School of Integrated Sciences for Life, Hiroshima University, 1-3-1 Kagamiyama, Higashi-Hiroshima, Hiroshima 739-8526, Japan.
*Present address: Division of Adaptation Physiology, School of Medicine, Faculty of Medicine, Tottori University, 86 Nishi-cho, Yonago, Tottori 683-8503, Japan.
‡Present address: Amphibian Research Center, Hiroshima University, 1-3-1 Kagamiyama, Higashi-Hiroshima, Hiroshima 739-8526, Japan.
§These authors contributed equally to is work

¶Author for correspondence (takeuchi@tottori-u.ac.jp)

T.T., 0000-0001-9308-1302; K.A., 0000-0002-5195-2576

Handling Editor: Patrick Tam
Received 27 October 2021; Accepted 21 January 2022

Development (2022) 149, dev200282. doi:10.1242/dev.200282

studies have reported that CRISPR/Cas9 is effective in amphibians such as axolotls and *Xenopus* (for example, Flowers et al., 2014; Sakane et al., 2018).

We developed a molecular genetic system for Iberian ribbed newts (*Pleurodeles waltl*), which have the remarkable ability to regenerate many tissues, including limbs (Hayashi et al., 2013). We recently established a highly efficient gene knockout system using CRISPR/Cas9 that enables us to mutate a target gene in the whole body and almost all alleles (more than 99%) in F0 animals (Suzuki et al., 2018), probably owing to the longer time for the first cleavage in *P. waltl* fertilized eggs. We can also disrupt multiple genes in F0 animals by the injection of multiple guide (g)RNAs and analyze their functions without crossing newts. We also performed a comprehensive analysis of the *P. waltl* transcriptome, and established gene models for almost all protein-coding genes in *P. waltl*, including Hox genes (Matsunami et al., 2019).

In the present study, we analyzed the functions of Hox13 paralogs during limb development and regeneration in newts using our CRISPR/Cas9 system. Newts have four Hox13 paralogs (*Hoxa13*, *Hoxb13*, *Hoxc13* and *Hoxd13*).We produced single, double, triple and quadruple Hox13 paralog mutants. We showed that Hox13 genes are essential for digit formation during development, as in mice. In addition, unlike in mice, *Hoxa13* plays a predominant role in digit formation. Finally, Hox13 genes are also required for digit formation in limb regeneration. These results indicate that the general function of Hox13 genes is conserved between limb development and regeneration, and across tetrapod taxa. In addition, the predominance of *Hoxa13* in newts has significant implications for the evolution of appendages.

RESULTS

Expression of newt Hox13 genes in limb development and regeneration

A comprehensive analysis of the *P. waltl* transcriptome revealed that *P. waltl* has at least three Hox13 paralogs (*Hoxa13*, *Hoxc13* and *Hoxd13*), and transcripts of these three genes were identified in the limb blastemas. We also found transcripts showing high homology with *Hoxb13* of the palmate newt (*Lissotriton helveticus*, GenBank: DQ158059) and axolotl (*Ambystoma mexicanum*, GenBank: AF298184.1) in *P. waltl* transcriptome data (Matsunami et al., 2019).

We first examined the mRNA expression of all four Hox13 paralogs (*Hoxa13*, *Hoxb13 Hoxc13* and *Hoxd13*) by RT-PCR in the forelimb (stage 40, the stage when the fourth digit is initially formed) and forelimb blastemas (two-digit stage) (Fig. S1). The expression of *Hoxa13*, *Hoxc13* and *Hoxd13*, but not *Hoxb13*, was detected in both developing limbs and blastemas (Fig. S1). The data from blastemas are consistent with those in *P. waltl* transcriptome data (Matsunami et al., 2019).

Next, we analyzed the expression patterns of *Hoxa13*, *Hoxc13* and *Hoxd13* in developing forelimbs using whole-mount *in situ* hybridization (WISH) to detect the spatiotemporal expression patterns of these genes. Forelimb buds are observed from stage 33 (st33) embryos (Shi, and Boucaut, 1995). At this stage, the expression of *Hoxa13* and *Hoxc13*, but not that of *Hoxd13*, could be detected in the whole limb bud mesenchyme (Fig. 1A,C). Whereas *Hoxa13* expression was gradually restricted to the distal region, *Hoxc13* expression was still detected in the whole limb buds except the cartilage primordia (humerus, radius, ulna and digits) (Fig. 1A, st36-38). *Hoxd13* expression was first observed at the distal posterior region at st36 (Fig. 1A, st36), and the pattern was maintained at later stages (st37 and 38). *Hoxd13* expression was not detected in the distal anterior margin corresponding to the digit I-forming region at st37 and 38 (Fig. 1A,C). The expression patterns of *Hoxa13* and *Hoxd13* were similar to those of the axolotl, another urodele amphibian (Bickelmann et al., 2018; Gardiner et al., 1995; Roensch et al., 2013; Woltering et al., 2019).

We next examined the expression patterns of *Hoxa13*, *Hoxc13* and *Hoxd13* in forelimb blastemas (late blastema and three-digit stages) using *in situ* hybridization on sections. Of the three genes, only *Hoxa13* expression could be clearly detected at the late blastema stage. Its expression was observed in the distal mesenchymal region (Fig. 1B, arrowheads; see also Fig. 1C). *Hoxa13* expression was also detected in the digit-forming region at the three-digit stage. Weak *Hoxd13* expression could be detected in the posterior region of the autopod at the three-digit stage (Fig. 1B, arrowheads; see also Fig. 1C). *Hoxc13* expression was indistinguishable from the background signal in all stages (Fig. 1B). The spatiotemporal expression patterns of *Hoxa13* and *Hoxd13* were very similar to those in developing limbs (Fig. 1A) and also to those in regenerating limbs of axolotls (Gardiner et al., 1995; Roensch et al., 2013).

Knockout of Hox13 genes in newts

We disrupted all Hox13 paralogs using a CRISPR/Cas9 system to investigate the function of Hox13 genes in limb development and regeneration. Although *Hoxa13*, *Hoxc13* and *Hoxd13*, but not *Hoxb13*, were expressed in the forelimbs during development and regeneration (Fig. 1, Fig. S1), it cannot be excluded that *Hoxb13* starts to be expressed and compensates for Hox13 functions in knockout (KO) animals in which Hox13 genes other than *Hoxb13* were disrupted.

In order to produce single, double, triple and quadruple compound mutants, we designed nine gRNAs (Fig. 2, Table 1). All gRNAs except G25 recognize homeobox sequences. The G25 target sequence is located around the splicing acceptor of exon 2 in *Hoxd13*. Most of the gRNAs recognize only one paralog; however, G22 and G27 recognize three and four paralogs, respectively, by use of common sequences in Hox13 homeoboxes (Fig. 2). To avoid the misreading of phenotypes due to off-target effects, each Hox13 paralog gene was targeted by two to five different gRNAs (Fig. 2, Table 1). The ribonucleoprotein complexes (RNPs), containing Cas9 and a gRNA or multiple gRNAs, were injected into fertilized eggs. Table 1 shows groups of F0 animals (hereafter referred to as crispants). For example, only *Hoxa13* was targeted in *a* crispant groups (*a-1* and *a-2*). The gRNAs used were different between *a-1* and *a-2* (Table 1). In *ac* and *ad* crispants, *Hoxa13/Hoxc13* and *Hoxa13/Hoxd13* were doubly targeted, respectively. Similarly, in *acd* and *abcd* crispants, *Hoxa13/Hoxc13/Hoxd13* and all four paralogs were multiply targeted, respectively (Table 1).

We obtained genomic DNAs from the tail fins of crispants at 2 months post-fertilization (mpf) and performed amplicon sequencing by next-generation sequencing (NGS) for genotyping. Genomic DNAs of Hox13 genes of 2-16 newts in each crispant group were investigated (Tables S1-S5). In total, 14 target sites, 51 crispants and 107 amplicons were analyzed. All target sites were mutated with high efficiency (mean±s.d., 97.4±2.3% in a total of 14 target sites; 96.7±5.4% in a total of 107 amplicons) (Table S1). Mutations by all gRNAs except G25 yielded deletions and/or insertions causing either frameshift mutations or deletions of amino acid residues in the homeodomains (Tables S2-S5). Because G25 also caused a deletion around the splicing acceptor of exon 2 in *Hoxd13* (Table S3, *ad-1*), the mutations might have caused splicing abnormalities. Thus, the genotyping strongly suggested that target Hox13 genes were disrupted in almost all Hox13 crispants.

Development (2022) 149, dev200282. doi:10.1242/dev.200282

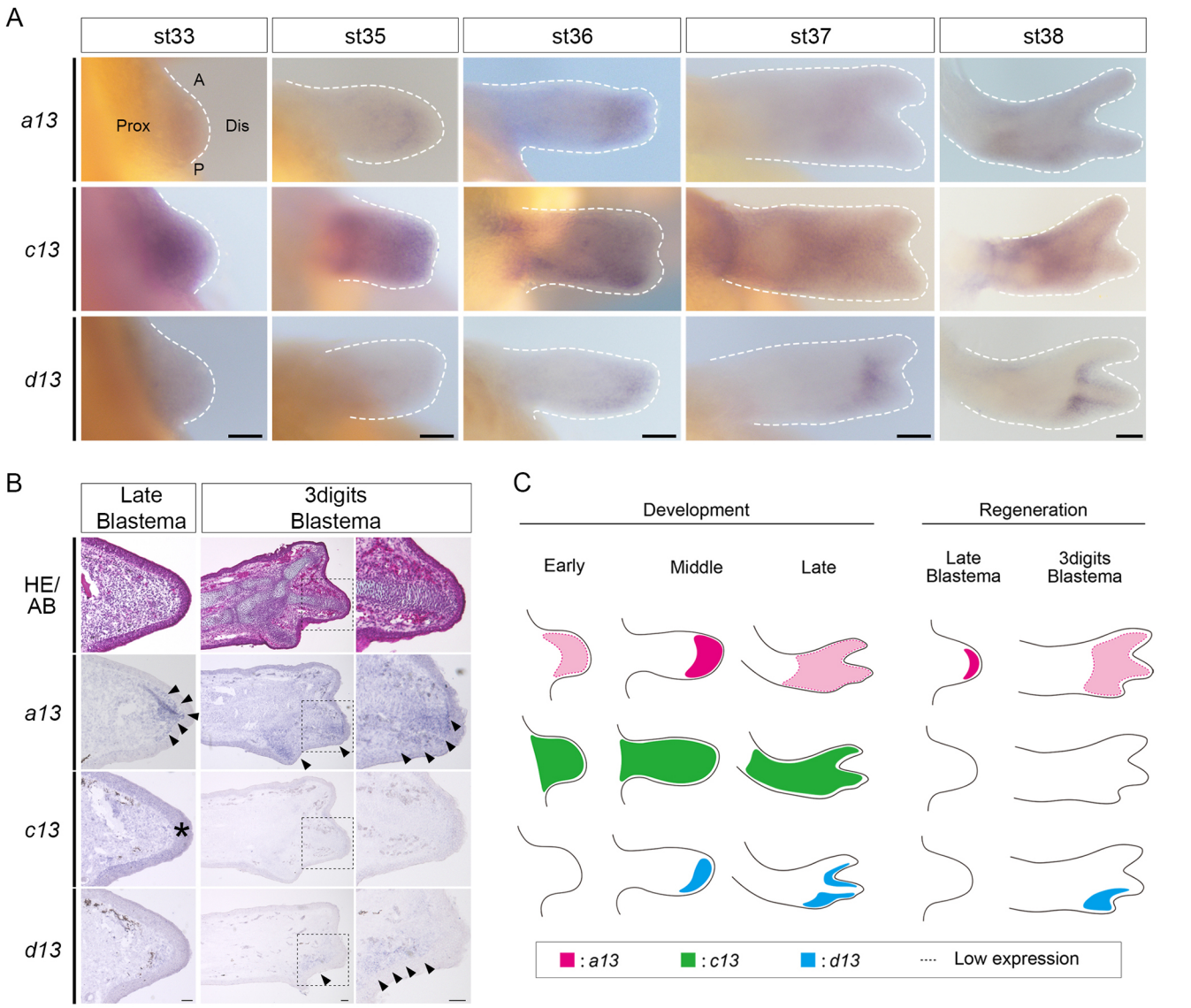

Fig. 1. Hox13 paralog expression in *P. waltl* forelimb development and regeneration. (A) The expression of Hox13 paralogs during forelimb development was visualized by WISH. White dashed lines show outlines of limb buds. A, anterior; Dis, distal; P, posterior; Prox, proximal. Scale bars: 100 µm. (B) The expression of Hox13 paralogs in blastemas during forelimb regeneration was visualized by *in situ* hybridization. The forelimbs of newts (2-3 mpf) were amputated at the most proximal region in the stylopod, and the blastemas at 16 days (late blastema) and 23 days (three digits blastema) post-amputation were examined. HE/AB, Hematoxylin-Eosin and Alcian Blue staining. Arrowheads and asterisk indicate positive signals and background signal in the epidermis, respectively. Dashed squares in the middle panels indicate the magnified regions on the right. Scale bars: 100 µm. (C) Schematic of *Hoxa13*, *Hoxc13* and *Hoxd13* expression patterns in the forelimb during development and regeneration. Expression was low in the regions surrounded by dotted lines. See also Fig. S1.

Hox13 genes have essential functions in the digit development of *P. waltl*

To investigate the function of Hox13 genes in limb development, we analyzed the phenotypes of the forelimbs of Hox13 crispants (Fig. 3, Fig. S2). All forelimbs of uninjected siblings (wild-type animals, n=206) had normal limb structures (Fig. 3A, Wt). Bone staining of limbs in all groups showed that the stylopod and zeugopod bones formed and appeared to be normal (Fig. 3A, Fig. S2). Whole autopod structures of all newts in *c* and *d* (*d-1* and *d-2*) crispant groups were normal (Fig. 3A, Fig. S2A). The autopods of all newts in all other crispant groups showed abnormalities both in the digits and in the carpal elements. The phenotypes of digits and carpal elements are described below.

Almost all newts in all crispant groups other than *c* and *d* lacked apparent digit structures (Fig. 3A, Fig. S2A), although a few crispants had one to three digits. Some crispants had cartilaginous phalange-like projections (for example, Fig. 3B, *a-2*, arrowheads). Therefore, we classified the digit phenotypes into five groups: normal, normal structure; class 1, three or two digits; class 2, one digit; class 3, one digital phalange-like projection; class 4, no digit structure (neither phalanges nor metacarpal bones) (Fig. 4A; for class 3 and 4, also see *a-2* and *ad-3/acd*, respectively, in Fig. 3B). The digits of almost all forelimbs of *a* (*a-1* and *a-2*) crispants showed class 3 and 4 phenotypes (97.2% in a total of 36 forelimbs of *a-1* and 80.0% in a total of 15 forelimbs of *a-2*) (Fig. 4B). Phenotypes of *ad* (*ad-1*, *ad-2* and *ad-3*) crispants were more severe than those of *a* (*a-1* and *a-2*) because the percentages of class 4 (no digit structure) increased significantly (P<0.05 in all combinations, Fisher's exact tests) (Fig. 4B). Phenotypes of *abcd* (*abcd-1* and *abcd-2*) crispants appeared to be slightly more severe than those of

Development (2022) 149, dev200282. doi:10.1242/dev.200282

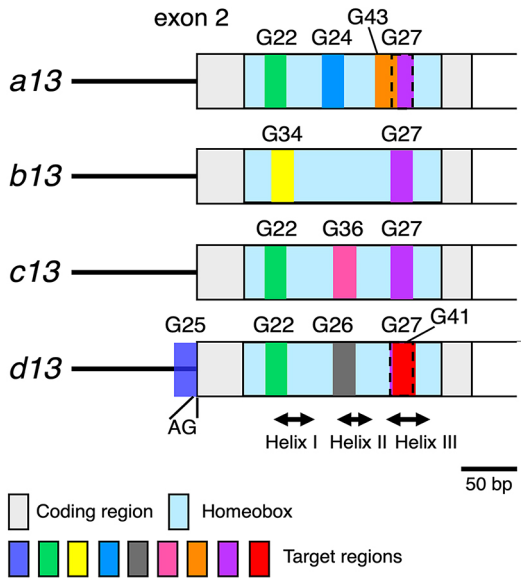

Fig. 2. Target regions for CRISPR/Cas 9-mediated gene disruption. Schematic of the regions targeted by CRISPR RNAs (G22-G43, Table 1, Table S1) in Hox13 genes. AG in *Hoxd13* indicates the consensus AG sequence in the 3′ splice site of the first intron.

ad (Fig. 4B), because there were no class 1 and 2 forelimbs. *ac* and *acd* crispants appeared to show similar phenotypes to *a* crispants (*a-1* and *a-2*) and *ad* crispants (*ad-1*, *ad-2* and *ad-3*), respectively (Fig. 4B). These results showed that disruption of *Hoxd13* had a synergistic effect on the *Hoxa13* single mutation, whereas that of *Hoxc13* did not on the *Hoxa13* single or *Hoxa13*/*Hoxd13* double mutations for digit formation. Observation of forelimb development in class 4 showed the elongation of limb buds, but no digits were formed (for *abcd-1* and *abcd-2*, Fig. 4C).

The morphology of carpal elements in class 3 and 4 forelimbs (almost all crispants in all crispant groups other than *c* and *d*) were also abnormal, and the numbers of carpal elements decreased compared with wild-type animals, *c* and *d-1* crispants (Fig. 3). Although the morphology was abnormal, the presence of carpal elements, unlike digits, in *abcd-1* and *abcd-2* crispants (Fig. 3A, Fig. S2A), in which all Hox13 paralogs were disrupted, indicated that carpal elements can develop without any Hox13 genes. They also had different phenotypes from the digits; the numbers of carpal elements seemed not to differ among *a-2*, *ac* and *ad-3* crispants, whereas those of *acd* and *abcd* crispants appeared to be fewer than those of *a-2*, *ac* and *ad-3* crispants (Fig. 3, Fig. S2; for examples, see *a-2*, *ad-3* and *acd* in Fig. 3B).

Taken together, we conclude that newt Hox13 genes have essential roles in digit formation and are necessary for the normal development of carpal elements. In particular, *Hoxa13* has a predominant function in digit formation. And whereas *Hoxc13* and *Hoxd13* are not indispensable for digit formation, *Hoxd13* has some functions in digit formation that probably complement *Hoxa13* function, even if only slightly.

Table 1. Crispant groups and their target genes

Name of crispant group	Target gene	gRNA	Position
a-1	*Hoxa13*	G24	HII
a-2	*Hoxa13*	G43	HIII
c	*Hoxc13*	G36	HII
d-1	*Hoxd13*	G26	HII
d-2	*Hoxd13*	G41	HIII
ac	*Hoxa13* and *Hoxc13*	G24 and G36	HII
ad-1	*Hoxa13* and *Hoxd13*	G24 and G25	HII and 3′ SS
ad-2	*Hoxa13* and *Hoxd13*	G24 and G26	HII
ad-3	*Hoxa13* and *Hoxd13*	G41 and G43	HIII
acd	*Hoxa13*, *Hoxc13* and *Hoxd13*	G22	HI
abcd-1	*Hoxa13*, *Hoxb13*, *Hoxc13* and *Hoxd13*	G22 and G34	HI
abcd-2	*Hoxa13*, *Hoxb13*, *Hoxc13* and *Hoxd13*	G27	HIII

HI-HIII, helix I-III; 3′ SS, 3′ splicing site.

Gene expression patterns in Hox13 crispants

Next, we investigated the expression patterns of several genes to examine their contribution to limb development in Hox13 crispants. The expression of *Shh*, a key regulator of anterior-posterior patterning, is regulated by Hoxa and Hoxd genes (Kmita et al., 2005), and is activated directly by Hox13 (Capellini et al., 2006; Galli et al., 2010). Its expression was detected in the posterior region of forelimb buds of *a-1* and *ad-2* crispants. Although the patterns were similar to that of wild-type newts, the intensity decreased (Fig. 5A), suggesting regulation of *Shh* by Hox13 in the newt limb. The expression of *Hoxd11* was observed in the middle region of the limb buds in wild-type animals at st35. However, the expression pattern slightly shifted to the distal region in *a-1* crispants (Fig. 5A). In *ad-2* crispants, the expression shifted more distally than that in *a-1* crispants (Fig. 5A). Shifts of *Hoxd11* expression have been reported in the limb buds of *Hoxa13* KO mice (Bastida et al., 2020). In addition, a shift and expansion to the distal region of *Hoxa11* expression have been observed in *Hoxa13* single and *Hoxa13*/*d13* double KO mice, respectively (Sheth et al., 2014). The shifts of *Hoxd11* expression in newts suggested the reduction of the presumptive autopod region or ectopic expression of *Hoxd11* in presumptive autopod cells. If the former is the case, then the zeugopod was in the most distal region. We also examined *Hoxd13* expression in *a-1* crispants. Unexpectedly, *Hoxd13* expression was not detected in *a-1* crispants (Fig. 5A). qRT-PCR analysis also showed a significant decrease of *Hoxd13* in *a-1* crispants (Fig. 5B).

These results suggest that Hox13 genes regulate the expression of *Shh* and are required for the generation or maintenance of the normal autopod region in newt limb buds, and that *Hoxa13* strongly regulates the expression level and pattern of *Hoxd13*.

Newt *Hoxd13* has functions in digit formation

Our analyses above showed that newt *Hoxd13* is not indispensable for limb development, and we could not obtain any clear data showing its functions in the limb development of newts. We had expected to infer the functions of *Hoxd13* by analyzing the phenotypes of *a* crispants; however, this was not possible because the *Hoxd13* expression level was strongly decreased in *a* crispants (Fig. 5). Therefore, we analyzed its functions directly by the induction of *Hoxd13* expression in limb buds of *a* crispants, in which almost no digit structure was formed.

For this purpose, we induced the expression of both *Hoxd13* and *GFP* or only *GFP* (control) by heat-shock treatment in *a-1* crispants (Fig. 6A). Because *Hoxd13* expression was initiated at st35-36 in the forelimb (Fig. 1A), we started heat shock at st34-35 (Fig. 6B). We examined only the limbs in which GFP florescence was observed after the heat shock.

Almost all forelimbs of control *a-1* crispants in which only *GFP* expression was induced showed class 3 or 4 phenotypes (one digital

Development (2022) 149, dev200282. doi:10.1242/dev.200282

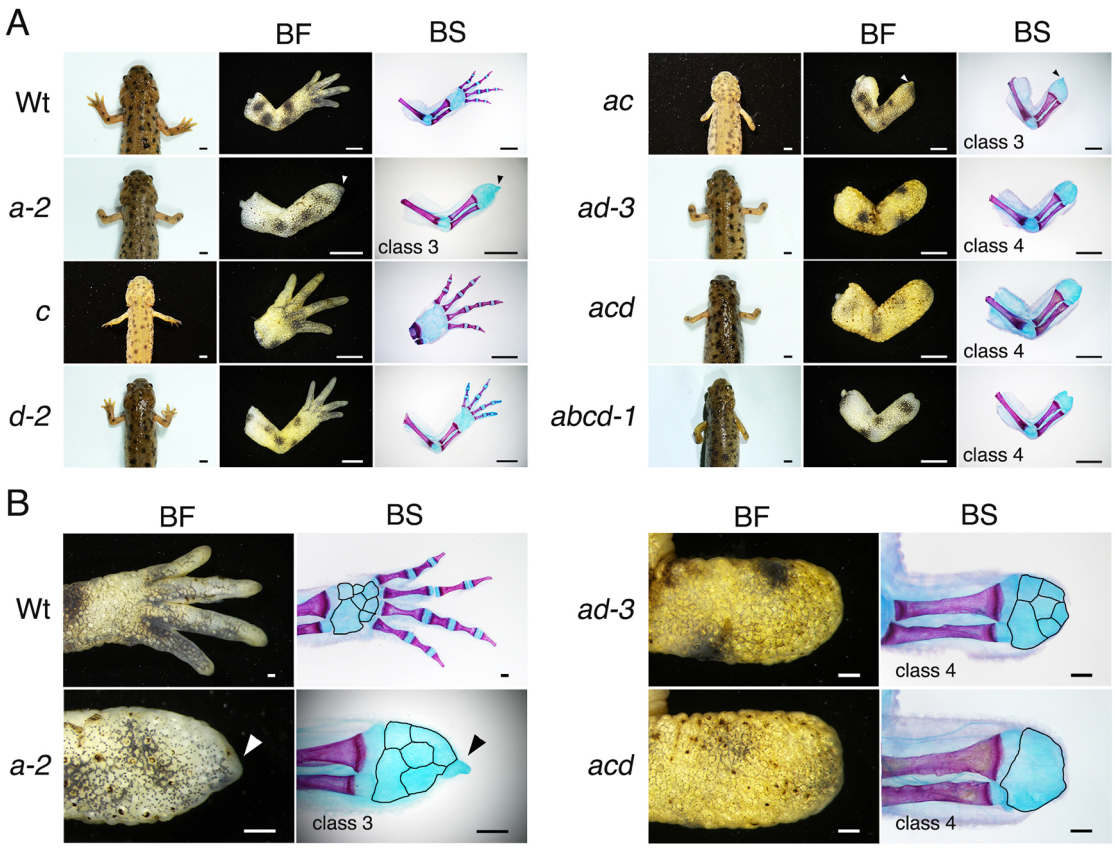

Fig. 3. Newt Hox13 genes have essential functions in digit formation during development. (A) Left: Dorsal views of representative wild-type (Wt) and Hox13 crispants (*a-2*, *c*, *d-2*, *ac*, *ad-3*, *acd* and *abcd-1*) at 3 mpf. BF and BS: Dorsal views of bright-field (BF) and bone staining (BS) patterns of representative developed forelimbs. Arrowheads in *a-2* and *ac* crispants represent digital phalange-like projections. Anterior, up. Scale bars: 2 mm. (B) Dorsal magnified views of representative developed right forelimbs of Wt (normal), *a-2* (class 3), *ad-3* (class 4) and *acd* (class 4) crispants. For classification, see Fig. 4A. The arrowheads in *a-2* crispants indicate one digital phalange-like projection. Black lines in BS show outlines of carpal elements. Anterior, up. Scale bars: 0.5 mm. See also Fig. S2.

phalange-like projection or no digit structure) (Fig. 6C,D). In contrast, after induction of *Hoxd13* expression in the forelimbs, limbs showing class 1 or 2 phenotypes (one to three digits) appeared and accounted for 40% of all limbs (Fig. 6C,D). The difference between only *GFP* and *Hoxd13* expression experiments was significant (Fisher's exact test, P=0.02).

These results showed that newt *Hoxd13* has functions in digit formation, but the function seemed to disappear or be very low in *a* crispants, probably because its expression was downregulated. These results also showed that knockout of *Hoxa13* can be rescued by the paralogous gene *Hoxd13*.

Hox13 genes are essential for digit formation in limb regeneration

Next, we examined Hox13 functions in limb regeneration. Hox13 crispants grew and metamorphosed, although some crispants died. Notably, *abcd-1* and *abcd-2* showed lower survival rates than other crispant groups, and only two animals survived in each group for unknown reasons. The forelimbs of uninjected siblings (wild type) and some surviving crispants after metamorphosis (3 mpf) were amputated at the proximal region in the stylopod. The autopod cells in Hox13 crispants other than in *c* and *d* groups became abnormal during development. Therefore, regeneration by amputation at the autopod would be from cells that were already abnormal and would not be appropriate for studying the function of Hox13 genes in limb regeneration. However, because the stylopods of Hox13 crispants were considered to be normal (Fig. 3, Fig. S2), and all distal regions were reconstructed from dedifferentiated stylopod cells by amputation at the stylopod, we thought it was feasible to examine the functions of Hox13 genes in limb regeneration by amputation at the stylopod. The forelimbs of class 3 or 4 were amputated in *a* and *ac* crispants. In the case of *ad*, *acd* and *abcd* crispants, the forelimbs of class 4 were analyzed (Fig. 3, Fig. S2).

The external appearance and bone staining showed that almost all regenerates in wild-type animals and *c* and *d* crispants had normal morphology (Fig. 7A, Fig. S3). A small number of these animals, including wild types, showed full or partial defects in the digits, mainly in digit III, probably as a result of errors in regeneration (class 1 in Fig. 7C). Almost all regenerates of *ad*, *acd* and *abcd* crispants showed class 4 phenotypes similar to development (Figs 4B, 7C). During limb regeneration of the class 4 regenerates, no apparent phenotypes were observed before the notch stage compared with wild types (Fig. S4, 1-18 days post-amputation; Movie 2); however, neither the notch structure nor digit formation was observed thereafter (Fig. S4, 21-39 days post-amputation; compare Movie 2 with Movie 1). Interestingly, phenotypes in *a* crispants became slightly weaker than those from initial limb development. The majority of forelimbs in class 3 or 4 (80% and 60% in *a-1* and *a-2*, respectively) moved to class 2 (Fig. 7C). These regenerates in class 2 had one digit-like structure with one or two phalange bones that could be stained with Alizarin Red (for example, Fig. 7B, *a-2*, arrows; compare with Fig. 3B, *a-2*, arrowheads). Similar structures were also observed in *ac* crispants (Fig. 7A, *ac*, arrows). The numbers and morphology of carpal

Development (2022) 149, dev200282. doi:10.1242/dev.200282

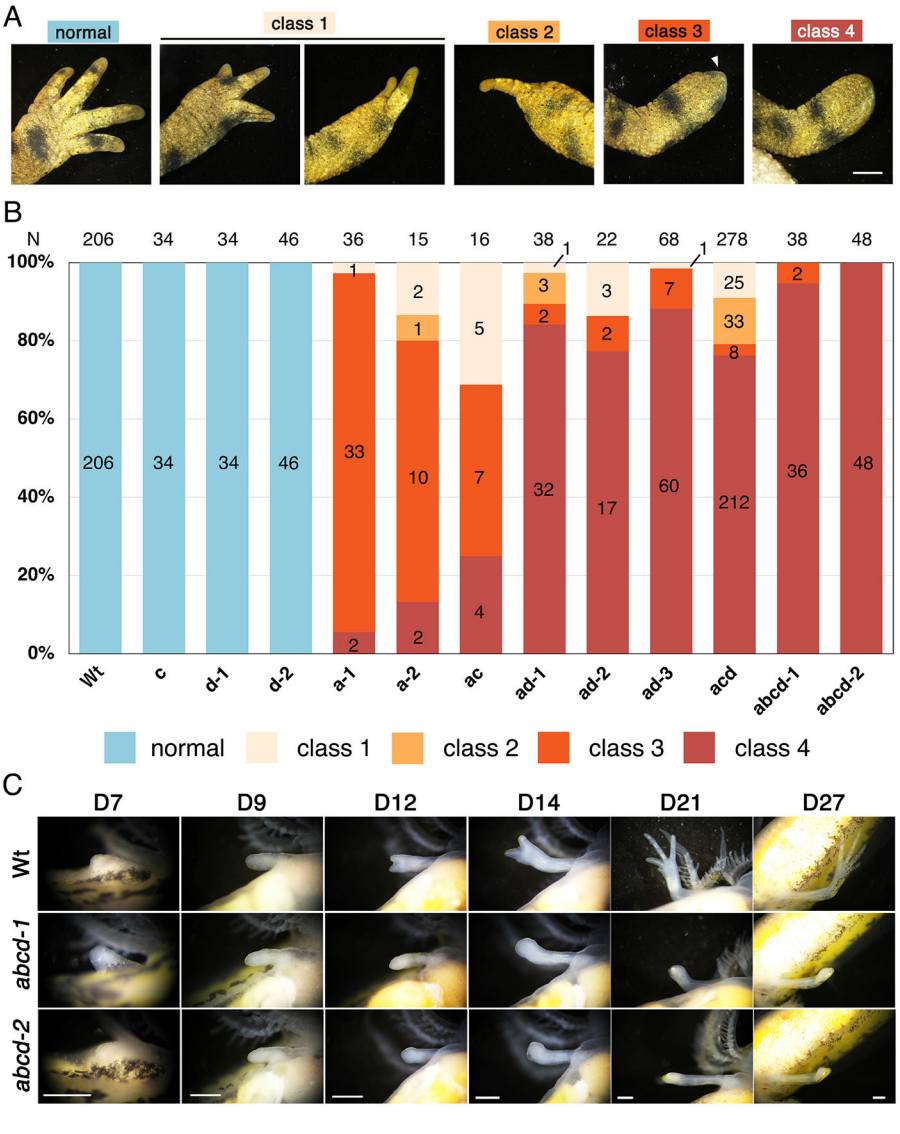

Fig. 4. Classification of digit phenotypes and development patterns of forelimbs in Hox13 crispants. (A) Dorsal views of representative forelimbs showing each class. Normal: normal four digits; class 1: three or two digits; class 2: one digit; class 3: one digital phalange-like projection (arrowhead); class 4: no digit structure. For class 3 and 4, see also the bone staining patterns in Fig. 3B. Anterior, up. Scale bar: 2 mm. (B) Distribution patterns of classes in each crispant group after development. Total number of forelimbs examined (N) and each class's number of forelimbs are indicated at the top and middle of each class, respectively. (C) Development of right forelimbs of a wild-type (Wt) embryo and *abcd* crispants. Limbs at 7-27 dpf are shown. Ventral (D7) and dorsal views (D9-D27). Anterior, up (D7-D14), right (D21) and left (D27). Scale bars: 1 mm.

elements did not show apparent changes compared with development in any group (Figs 3, 7A,B).

Overall, these results showed that Hox13 genes are essential for digit formation in limb regeneration. As with development, *Hoxa13* had a predominant function in digit formation during regeneration.

The predominant role of *Hoxa13* in digit formation is confirmed by analysis of germline mutants

Finally, in order to confirm the predominant role of *Hoxa13* in digit formation, we examined whether Hox13 germline mutants showed the same phenotypes as in crispants.

We generated *Hoxa13* and *Hoxc13* mutants by intercrossing F1 animals ($Hoxa13^{+/\Delta 40}$, $c13^{+/\Delta 6}$×$Hoxa13^{+/\Delta 40}$, $c13^{+/\Delta 6}$; for details, see 'Materials and methods'). The sequence of an *Hoxa13* mutant allele showed the deletion of 40 nucleotides in the homeobox, indicating that the allele was null because of a large deletion and frameshift (Fig. 8A).

The developed forelimbs of *Hoxa13* mutants ($a13^{\Delta 40/\Delta 40}$) showed mainly class 3 or 4 phenotypes (for an example of class 3, Fig. 8B). Similar results were also shown for other alleles ($a13^{\Delta 40/\Delta\sim 1000}$, Fig. S5; for details, see 'Materials and methods'). The distribution pattern of the class of all *Hoxa13* mutants ($a13^{\Delta 40/\Delta 40}$ and $a13^{\Delta 40/\Delta\sim 1000}$) was similar to that of *a* crispants (Figs 4B, 8C). By contrast, no abnormalities were observed in the digit formation of $Hoxc13^{\Delta 6/\Delta 6}$ newts (Fig. 8B,C).

We also obtained *Hoxd13* germline mutants by intercrossing F1 animals ($Hoxd13^{+/\Delta 15}$×$Hoxd13^{+/\Delta 13}$; for details, see 'Materials and methods'). No $Hoxd13^{\Delta 13/\Delta 15}$ newts showed abnormalities in digit formation (Fig. S6). In addition, we obtained *Hoxd13* germline mutants with other alleles by intercrossing *d-2* crispants (F0). All *Hoxd13* alleles were considered to be null in these F1 animals because of a deletion in the sequence coding homeodomain helix III, which binds to target DNAs (Fig. 8A). Moreover, $Hoxd13^{\Delta 6\text{-}1}$ and $Hoxd13^{\Delta 6\text{-}2}$ alleles had an abnormal stop codon and a deletion of codons coding for DNA-recognition residues in the Hox13-type homeodomain, respectively (Zhang et al., 2011) (Fig. 8A). These *Hoxd13* mutant newts showed no abnormalities in digit formation (Fig. 8B,C).

The *Hoxa13* mutants were also examined for their limb regeneration phenotypes. The regenerated forelimbs of $Hoxa13^{\Delta 40/\Delta 40}$ newts showed class 2-4 phenotypes (Fig. 8D), as were observed in *a* crispants (Fig. 7C).

These results are consistent with those in the crispants (Figs 3, 4, 7; Figs S2, S3), indicating that genome editing in newts is

Development (2022) 149, dev200282. doi:10.1242/dev.200282

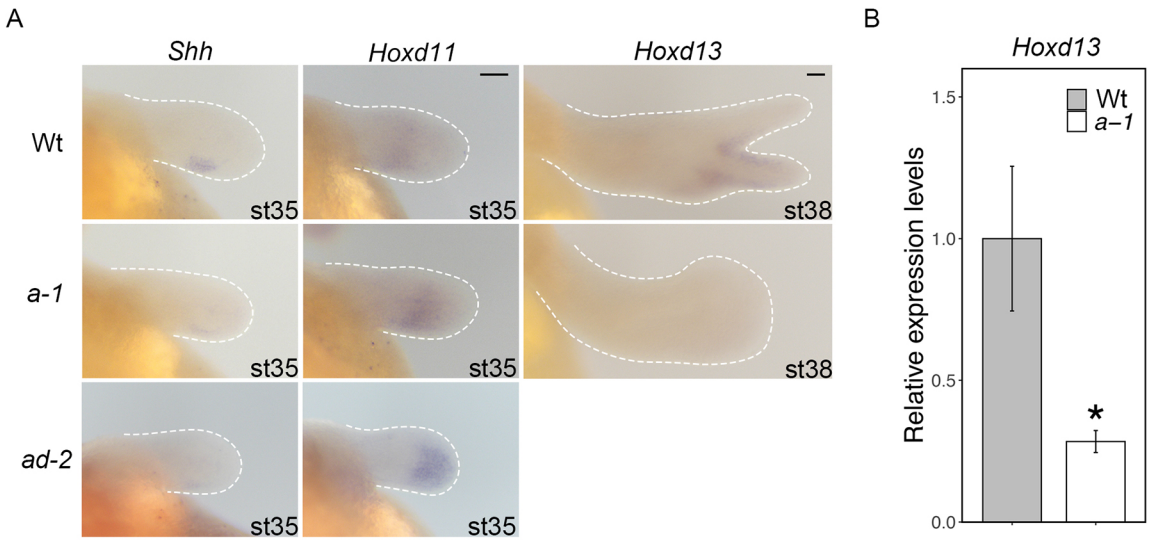

Fig. 5. Gene expression patterns in the forelimb buds of Hox13 crispants. (A) Expression patterns of *Shh*, *Hoxd11* and *Hoxd13* in the forelimb buds were visualized by WISH. White dashed lines show outlines of limb buds. Dorsal views are shown. Anterior, up. Scale bars: 100 µm. (B) mRNA levels of *Hoxd13* in forelimb buds of wild-type animals (Wt) and *a-1* crispants at st38 were analyzed by qRT-PCR. Expression levels relative to Wt are represented as mean±95% confidence interval for four mixtures. Each mixture contained six forelimb buds from three animals. **P*<0.001, versus Wt forelimbs (Welch's *t*-test).

extremely useful. Based on all these results, we concluded that newt *Hoxa13* plays a predominant role in digit formation in limb development and in regeneration.

DISCUSSION

The predominance of *Hoxa13* function in digit formation during development

Our analysis of Hox13 genes in newt limb development revealed two important findings. First, the role of Hox13 in digit formation during development is essential and conserved in both newts and mice (Fig. 3) (Fromental-Ramain et al., 1996b). Second, among the newt Hox13 paralogs, *Hoxa13* in particular plays a predominant role in digit formation. The evidence is that (1) *a* crispants and *Hoxa13* germline mutants lacked all digit structures other than one phalange-like piece; (2) *c* crispants, *Hoxc13* germline mutants, *d* crispants and *Hoxd13* germline mutants show no phenotypes; and (3) *Hoxb13* expression was not detected in the developing limbs (Figs 3, 4, 8; Figs S1, S2, S6). In contrast, mouse *Hoxa13* and *Hoxd13* have overlapping and mutually redundant functions, because major parts of digit structures remain in *Hoxa13* or *Hoxd13* single KO mice, although each has a specific phenotype such as the lack of digit I in the *Hoxa13* KO mouse (Dollé et al., 1993; Fromental-Ramain et al., 1996b). What makes newts and mice different? Their differences might not result from the protein functions of Hoxd13 for digit formation, because the induction of newt *Hoxd13* expression caused digit formation (Fig. 6).

We speculate that there are two major differences between mice and newts. One is the expression pattern of *Hoxd13* in the urodeles. Newt *Hoxd13* expression at least started at a later stage than that of *Hoxa13*, and the pattern in newts and axolotls is restricted to the distal posterior region, whereas *Hoxa13* was expressed broadly in the future autopod region, as in mice (Figs 1, 9A) (Bickelmann et al., 2018; Gardiner et al., 1995; Roensch et al., 2013; Satoh et al., 2006; Woltering et al., 2019). Conversely, in mice, *Hoxa13* and *Hoxd13* expression overlaps in a broad area of the future autopod region (Bastida et al., 2020; Dollé et al., 1993; Zákány et al., 2004; for a review, see Zákány and Duboule, 2007) (Fig. 9A), which enables the redundant function of the two genes. The other reason is that newt *Hoxd13* expression is strongly dependent on *Hoxa13* in the limb bud (Fig. 5). In mice, similar regulation is observed only in digit I (Bastida et al., 2020; Sheth et al., 2014). As a result of these expression patterns and the dependency on *Hoxa13*, mouse *Hoxd13* can form digits II-V independently of *Hoxa13*, whereas the independent function of newt *Hoxd13* is largely limited.

What causes the urodele-specific expression pattern of *Hoxd13*? It has been suggested that enhancer sharing has been disrupted by the expansion of the intergenic regions between *Hoxd11* and *Hoxd13* in axolotls (Meyer et al., 2021). This expansion may have resulted in a urodele-specific expression pattern of *Hoxd13* and the predominant role of *Hoxa13* in newt digit formation.

It is also interesting why there is a difference in the dependency of *Hoxd13* on *Hoxa13* between newts and mice. As described above, mouse *Hoxa13* regulates *Hoxd13* only in the future digit I region (Bastida et al., 2020; Sheth et al., 2014), whereas it regulates the newt gene in the whole autopod region (Fig. 5). Mouse Hoxa13 regulates *Hoxd13* expression by attenuating *Gli3* transcription directly (Bastida et al., 2020). However, it is still unknown why this regulation is limited only to the future digit I region and not limited in newts. It may be that other genes, such as 5′Hox, compensate for *Hoxa13* regulation of *Hoxd13* in the mouse autopod in regions other than that of future digit I, but not in the whole autopod of newts. Therefore, determining the expression and functions of these genes is important for understanding the differences between newts and mice. It is also intriguing how the dependency of *Hoxd13* on *Hoxa13* has diverged during evolution.

It is important to know whether and to what extent the predominant role of *Hoxa13* is related to the developmental pattern, morphology and functions of newt limbs, especially digits. Swapping of *Hoxa13* and *Hoxd13* genes between newts and mice or changing the *Hoxd13* expression pattern of one to that of the other are ideal experiments and would provide insights regarding the biological significance of the role of *Hoxa13* in newts.

The roles of newt Hox13 genes in limb regeneration

To what extent regeneration is similar to development and which events are specific for development or regeneration have long

Development (2022) 149, dev200282. doi:10.1242/dev.200282

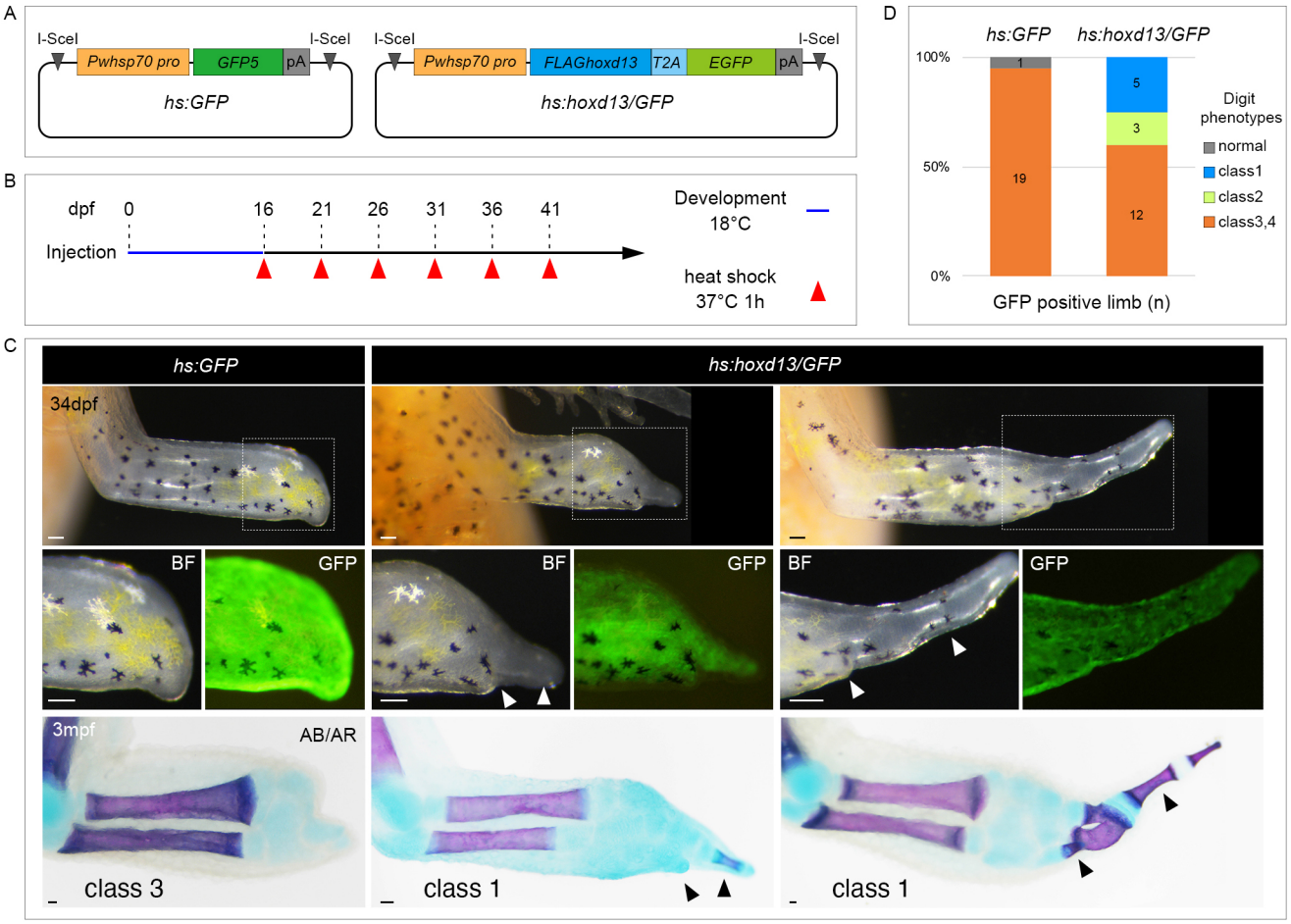

Fig. 6. Newt *Hoxd13* has functions in digit formation. (A) Schematic of injected plasmids. Left: Control plasmid for the induction of only GFP (*hs:GFP*). Right: Plasmid for the induction of *P. waltl Hoxd13* and *GFP* (*hs:Hoxd13/GFP*). In addition to each plasmid, RNPs containing G24 gRNA were injected into eggs to disrupt *Hoxa13*. (B) Experimental scheme for *GFP* and *Hoxd13* induction. Embryos were repeatedly heat-shocked (red arrowheads) every 5 days from 16 dpf to 41 dpf. (C) Digit phenotypes in GFP-positive forelimbs. Top: Dorsal, bright-field (BF) views of control limb (left: *hs:GFP*, class 1) and two representative limbs (middle and right: *hs:Hoxd13/GFP*, class 1). Middle: Magnified BF and GFP views of the distal regions of the boxed areas above. Bottom: (AB/AR): Alizarin Red and Alcian Blue bone staining pattern of each limb at 3 mpf. Arrowheads indicate individual digits. There are several Alizarin Red-positive phalanges. Both limbs had at least two digits. Anterior, up. Scale bars: 100 µm. (D) Percentage of limbs by class (see Fig. 4A). Numbers indicate number of limbs in each class.

been topics of discussion. In limbs, several factors have been shown to be regeneration specific. For example, signaling from neurons is necessary for blastema growth in limb regeneration (for a review, see Stocum, 2017), but not for limb bud growth in development. Although previous studies have suggested that the pattern formation of limbs is conducted in a similar manner during development and regeneration (for a review, see, Nacu and Tanaka, 2011), whether the same molecular system is used for both cannot be concluded, mainly because no functional analyses have been performed. 5′Hox genes are speculated to act in the same molecular system for patterning during limb development and regeneration.

Our results indicate that newt Hox13 genes are essential for digit formation during limb regeneration. This is the first finding not only of a Hox gene but also of any gene having the same function both in development and regeneration. It is worth noting that *Hoxa13* plays a predominant role in digit formation during limb regeneration as well as in development, showing that the general roles of Hox13 paralogs are conserved between the two processes.

We found no phenotypes that suggested regeneration-specific functions of Hox13, except for the minor phenotypes observed in *a* crispants (Fig. 7, Fig. S3). Phenotypes in *a* crispants became slightly weaker than those in limb development. Because this phenotypic change was not confirmed in a few of the *Hoxa13* germline mutants that we could analyze (Fig. 8D), the change needs to be investigated by using more germline mutants in the future.

The intercalation model theorizes a mechanism unique to limb regeneration but not to development (McCusker et al., 2015; Stocum, 2017). In one of the models for the initiation of urodele limb regeneration, the distalization at the tip of the stump, which follows limb amputation, triggers limb regeneration (Maden, 1977; for review, see Stocum, 2017). Here, the simultaneous expression of *Hoxa13* and *Hoxa9* within 24 h after amputation (Gardiner et al., 1995; Torok et al., 1998) is suggestive of early distalization. However, the expression pattern was not supported by analysis using antibodies against Hox proteins (Roensch et al., 2013). Our data here do not support the intercalation model in which Hox13 plays indispensable roles, such as in distalization at the tip of the stump, because limb regeneration itself progressed without Hox13 functions. However, our results cannot exclude the intercalation model based on other molecules, such as FGFs (Makanae and Satoh, 2018). Further detailed analyses of the expression and function of various genes required for the intercalation model are necessary to test it. Our studies have shown that a CRISPR/Cas9 system in newts is extremely useful for these analyses.

Development (2022) 149, dev200282. doi:10.1242/dev.200282

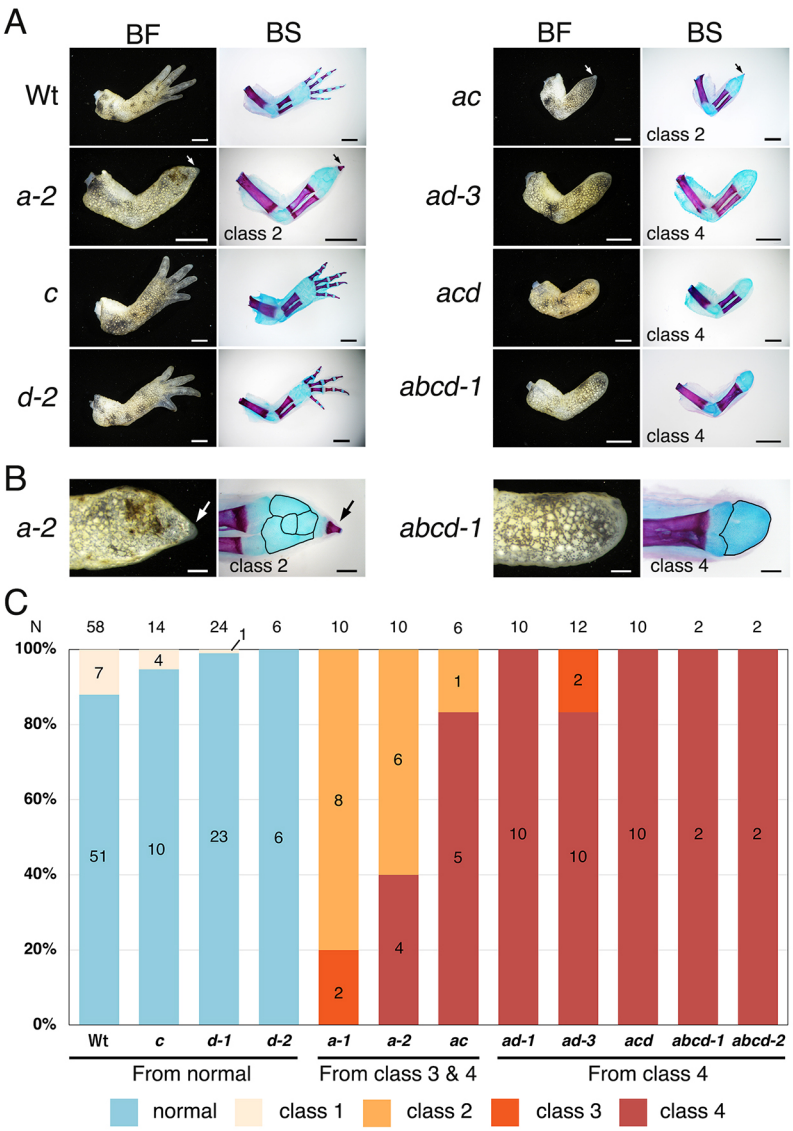

Fig. 7. Newt Hox13 genes have essential functions in digit formation during regeneration. (A) BF and BS: Dorsal views of bright-field (BF) and bone staining (BS) patterns of representative regenerated forelimbs. Representative phenotypes are shown. Limbs after 3 mpf were amputated at the most proximal region in the stylopod. Regenerates were fixed at 9 weeks post-amputation. Arrows in *a-2* and *ac* crispants represent digit-like structures with one or two phalange bones. Anterior, up. Scale bars: 2 mm. (B) Dorsal magnified views of representative regenerated right forelimbs of *a-2* (class 2) and *abcd-1* (class 4) crispants. For classification, see Fig. 4A. The arrowheads indicate phalange bones. Black lines in BS show outlines of carpal elements. Anterior, up. Scale bars: 0.5 mm. (C) Distribution patterns of classes in each crispant group after regeneration. Total number of forelimbs examined (N) and each class's number of forelimbs are indicated at the top and middle of each class, respectively. See also Figs S3 and S4.

Hox13 functions in vertebrate appendage evolution

In the evolution of limbs from ancestral fish fins, the acquisition of the autopod with digits is a crucial event. In primitive tetrapods, such as *Acanthostega*, the limbs were polydactyl (Coates, 1994), and a pentadactyl state was only stabilized in later tetrapods. 5′Hox genes are considered to play important roles in this evolutionary process (the fin-to-limb transition and changes in the dactyl state), and changes in the expression patterns and activities of these genes may be involved (for reviews, see Leite-Castro et al., 2016; Paço and Freitas, 2018; Schneider and Shubin, 2013; Tanaka, 2016; Woltering and Duboule, 2010). However, most studies on the role of 5′Hox genes in evolution using present-day animals have analyzed expression patterns, and functional analyses using genetics, such as KO experiments, have only been performed in mice and zebrafish. Of note, there have been no functional studies on amphibians, which were the first terrestrial tetrapods with digits. The present study is important because it helps fill this gap.

Our results and those of several other studies have led us to consider the following hypotheses (Fig. 9B). (1) The function of *Hoxd13* in the formation of the distal structures of appendages such as digits was not strong from fishes to amphibians. (2) However, the function of *Hoxa13* was consistently strong from fishes to amniotes.

The evidence for the above is as follows. First, KO studies of *hoxa13* and *hoxd13* in zebrafish have shown that zebrafish *hoxa13*, but not *hoxd13*, is necessary to form the fin ray, which is considered to share a common developmental history with the digits (Nakamura et al., 2016). Second, when only *Hoxa13* or *Hoxa11/a13* are active in mice, *Acanthostega*-like truncated digits with polydactyly are observed (Zákány et al., 1997). As an opposing phenotype, oligodactyly is observed in cases when only Hoxd genes are active. These results suggest that *Hoxa13*, but not *Hoxd13*, clearly functions in the polydactyly of tetrapods such as *Acanthostega*. Finally, in newts, our analysis showed that *Hoxa13*, but not *Hoxd13*, has essential functions in digit formation (*Hoxa13* predominance).

Analyses of expression patterns and functions of 5′Hoxd genes in mice and chickens (Yokouchi et al., 1991; Zákány and Duboule, 2007) suggest that late 5′Hoxd expression has important functions in digit formation in amniotes. Furthermore, a comparison of the expression patterns and enhancers mainly in mice and fishes provides a model in which quantitative and spatiotemporal changes

Development (2022) 149, dev200282. doi:10.1242/dev.200282

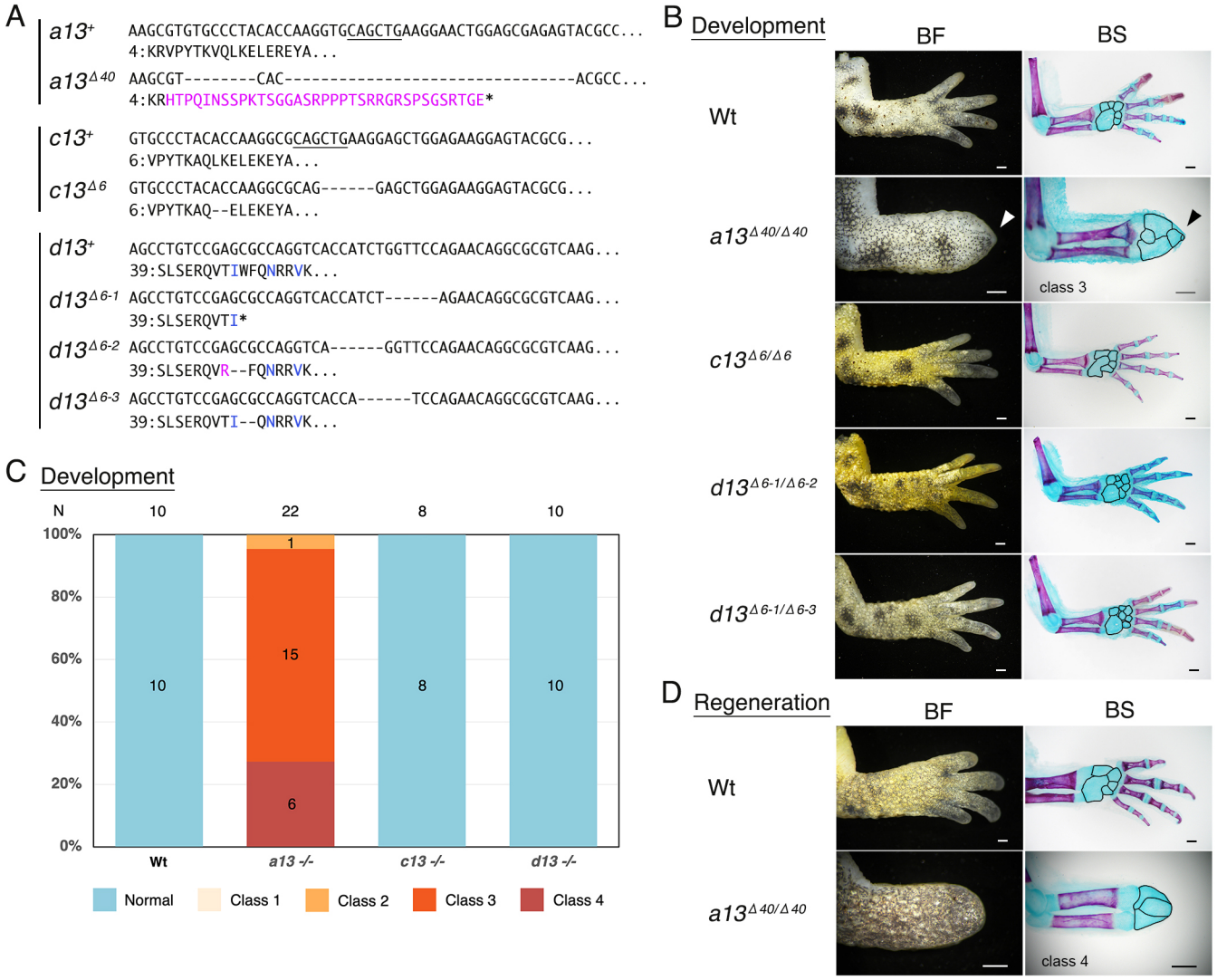

Fig. 8. The predominant role of *Hoxa13* in digit formation as confirmed by analysis of germline mutants. (A) Nucleotide and amino acid sequences of wild-type and mutant alleles. PvuII recognition sites used for genotyping are underlined. The numbers to the left of the amino acid sequences indicate the position of the first residue in the homeodomain. Magenta characters, blue characters, asterisks and dashes indicate sequences different from the wild type, DNA-recognition residues, 'stop', and deleted sequences, respectively. (B,D) BF and BS: Dorsal views of bright-field (BF) and bone staining (BS) patterns of representative developed (B) and regenerated (D) right forelimbs of *Hoxa13* (F2), *c13* (F2) and *d13* (F1) germline mutants. *Hoxd13* mutants were obtained by intercrossing *d-2* crispants. Arrowheads in a $Hoxa13^{\Delta 40/\Delta 40}$ mutant represent a digital phalange-like projection. Black lines in BS show outlines of carpal elements. For classification, see Fig. 4A. Anterior, up. Scale bars: 0.5 mm. (C) Distribution patterns of classes in each germline mutant group after development. Total number of forelimbs examined (N) and each class's number of forelimbs are indicated at the top and middle of each class, respectively. The $Hoxa13^{-/-}$ and $Hoxc13^{-/-}$ mutants were F2 animals, and their genotypes are ($Hoxa13^{\Delta 40/\Delta 40}$ and $Hoxa13^{\Delta 40/\Delta\sim 1000}$) and $Hoxc13^{\Delta 6/\Delta 6}$, respectively. The $Hoxd13^{-/-}$ mutants were F1 and F2 animals, and their genotypes are ($Hoxd13^{\Delta 13/\Delta 15}$, $Hoxd13^{\Delta 6\text{-}1/\Delta 6\text{-}2}$ and $Hoxd13^{\Delta 6\text{-}1/\Delta 6\text{-}3}$). See also Figs S5 and S6.

in late 5′Hoxd expression, as a result of modification or acquisition of late enhancers, may establish the autopodial area within the digital skeleton during fin-to-limb transition (for reviews, see Leite-Castro et al., 2016; Paço and Freitas, 2018; Schneider and Shubin, 2013; Tanaka, 2016; Woltering and Duboule, 2010). However, because in this model *Hoxd13* has main functions for digit formation among 5′Hoxd genes, and the predominant function of *Hoxd13* is necessary for digit acquisition, our hypotheses described above challenge this model.

If our hypotheses are correct, then the following scenario is possible. Some of the mechanisms required for autopod formation were already being used in fin morphogenesis (e.g. *Hoxa13* function for fin-ray formation). Then, the separation of the expression regions of *Hoxa11* and *Hoxa13*, which were insufficient in fishes, and the acquisition of a sufficient autopodial area, enabled the formation of an endochondral skeleton by *Hoxa13*. This was the first autopod in tetrapods and the initial stage of tetrapod digit morphogenesis. Digit formation by *Hoxa13* alone is unstable, as seen in the polydactyl state in several ancestors of amphibians. Extant amphibians still strongly retain this unstable state, and polydactyly can also be seen in some extant amphibians (Hayashi et al., 2015). Then, the stronger function of *Hoxd13* could have established the pentadactyl state in amniotes. It is still possible that newts may have independently acquired *Hoxa13* predominance, and further studies will be important to show *Hoxa13* predominance in other amphibians and sarcopterygians, and the function and expression of other 5′Hox genes in newts.

The present study and previous studies have shown that the Hox13 genes are essential for the formation of distal appendages (fin rays and digits) in mammals, amphibians and fish. Our studies also show that our newt-based analysis system can cover the gap

Development (2022) 149, dev200282. doi:10.1242/dev.200282

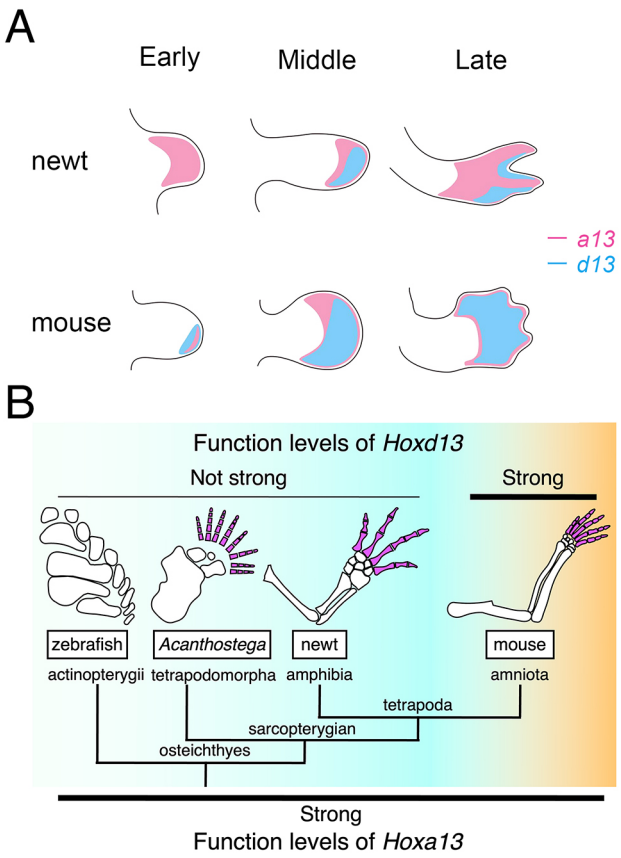

Fig. 9. Schema showing *Hox13* expression patterns and the predicted function levels during digit evolution. (A) *Hoxa13* (red) and *Hoxd13* (blue) expression patterns in the developing forelimb buds. The patterns of the newt and mouse were drawn with reference to Fig. 1B and published studies (Bastida et al., 2020; Dollé et al., 1993; Zákány et al., 2004), respectively. (B) Predicted *Hoxd13* (top) and *Hoxa13* (bottom) function levels during digit evolution.

between zebrafish and mice and is a new tool for investigating the roles of Hox genes in the development, regeneration and evolution of various organs.

MATERIALS AND METHODS

Newts

In this study, we used Iberian ribbed newts (*Pleurodeles waltl*) that were raised in our laboratory. The animals were reared as described previously (Hayashi et al., 2013). All procedures were carried out in accordance with the Institutional Animal Care and Use Committee of Tottori University (Tottori, Japan) and the national guidelines of the Ministry of Education, Culture, Sports, Science and Technology of Japan. Staging was performed as described in a previous study (Shi and Boucaut, 1995).

Preparation of RNPs and microinjection

gRNAs were designed using CRISPR-direct (Naito et al., 2015). Positions of the targets and the sequences are shown in Fig. 2 and Table S6, respectively. No gRNAs showed high identity with any other gene bodies according to *P. waltl* comprehensive transcriptome data, including the sequences of any other homeobox genes (Matsunami et al., 2019). At least two nucleotides were unmatched among the 20 nucleotides of the protospacer sequences, which further had PAM sequences at the 5′ or 3′ end. The target sequences of G22 and G26 had PvuII and SfoI cleavage sites, respectively (Table S6). The synthetic tracrRNA, gRNA and Cas9 protein were obtained from Integrated DNA Technologies (IDT). The tracrRNA and gRNA were annealed, and then RNPs, containing Cas9, were produced in accordance with the manufacturer's instructions just before injection. Microinjection of RNPs was performed based on our previous reports (Hayashi et al., 2019; Suzuki et al., 2018).

Germline mutants

We outcrossed *acd* crispants with wild-type newts. Because sufficient fertility was not observed in class 3 and 4 crispants, we used class 1 crispants. Double monoallelic F1 newts ($Hoxa13^{+/\Delta 40}$, $Hoxc13^{+/\Delta 6}$) were obtained and were intercrossed to obtain single homozygous biallelic mutants ($Hoxa13^{\Delta 40/\Delta 40}$ or $Hoxc13^{\Delta 6/\Delta 6}$). We also obtained $Hoxa13^{\Delta 40/\Delta\sim 1000}$ mutants by intercrossing $Hoxa13^{+/\Delta 40}$ and $Hoxa13^{+/\Delta\sim 1000}$ animals. The $Hoxa13^{+/\Delta\sim 1000}$ newts were generated from outcrossing *ad-2* crispants with wild-type newts. The $Hoxa13^{\Delta\sim 1000}$ allele had a large deletion (~1000 bp) around the G24 target region (Fig. S5). $Hoxd13^{\Delta 13/\Delta 15}$ mutants were obtained by intercrossing $Hoxd13^{+/\Delta 13}$ and $Hoxd13^{+/\Delta 15}$ animals, which were also generated from outcrossing *ad-2* crispants with wild-type newts. The sequences of $Hoxa13^{\Delta 40}$, $Hoxc13^{\Delta 6}$, $Hoxd13^{\Delta 13}$ and $Hoxd13^{\Delta 15}$ alleles are shown in Fig. 8A and Fig. S6. Genotyping of F2 animals was performed using PvuII (*Hoxa13*) or SfoI (*Hoxd13*) digestion of amplicons. The recognition sequence of the enzyme was mutated in these alleles (Fig. 8A, Fig. S6). For PCR amplification, the same primers as for NGS analysis, but without the barcoded overhang adapter sequence, were used (Table S7). In addition, we obtained $Hoxd13^{\Delta 6\text{-}1/\Delta 6\text{-}2}$ and $Hoxd13^{\Delta 6\text{-}1/\Delta 6\text{-}3}$ mutants by intercrossing *d-2* crispants (F0). The sequences of $Hoxd13^{\Delta 6\text{-}1}$, $Hoxd13^{\Delta 6\text{-}2}$ and $Hoxd13^{\Delta 6\text{-}3}$ alleles are shown in Fig. 8A. For genotyping, see 'Genotyping using NGS' below.

Plasmid constructions and transgenesis

To generate the plasmids *hs:GFP* and *hs*:*Hoxd13*/*GFP*, 0.6-kb genomic sequences upstream of the *P. waltl hsp70* and *P. waltl Hoxd13* open reading frame (ORF) fragments were amplified from wild-type *P. waltl* genomic DNA and cDNA using PCR with primers (Table S7). Heat-shock promoter (*Xenopus laevis*-type heat-shock promoter) sequences of the original plasmid (*hsp70*:*gene-P2A-EGFP*/I-SceI, a kind gift from Dr Yokoyama of Hirosaki University, Japan) were exchanged with the *P. waltl*-type (0.6-kb) using KpnI and BamHI sites. To ensure that the G24 gRNA targeting region of the *Hoxd13* ORF was not cleaved by the RNP, containing G24 gRNA, the PAM sequence was replaced with another sequence in which the codon was unchanged. In *hs*:*Hoxd13*/*GFP*, the T2A sequence was inserted at the 3′ site of the *Hoxd13* ORF (the stop codon was deleted) using the In-Fusion cloning system (Takara Bio). A FLAG tag was also inserted at the 5′ site of the *Hoxd13* ORF using PCR. To generate *hs:GFP* or *hs*:*Hoxd13*/*GFP* transgenic newts (F0) in which *Hoxa13* is disrupted, the I-SceI plasmid solution (300 ng of plasmids) digested with I-SceI (11.5 units, NEB) and an RNP containing G24 gRNA were mixed at a ratio of 1:1. The amount of total injection solution and plasmid was 18.4 nl and 138 pg, respectively, per egg. After injection, eggs were kept at 12°C for 3-6 h to delay the cleavages, and then kept at 15-16°C overnight. Injected embryos were incubated at 18°C until 16 days post-fertilization (dpf) to avoid leakage expression from the introduced constructs. At 16 dpf (st34-35), heat shock was performed by incubating embryos at 37°C for 1 h. Embryos were repeatedly heat shocked every 5 days until 41 dpf. After 16 dpf, embryos were raised at 25-26°C.

Genotyping using NGS

Genomic DNA was extracted from tail fins after 2 mpf. The target region was amplified from the lysates using KAPA HiFi enzyme (for NGS analysis, Roche Diagnostics) or KOD Fx Neo (TOYOBO) with primer sets (Table S7). Amplicons were obtained by primers containing barcoded overhang adaptor sequences according to a 16S Metagenomic Sequencing Library Preparation Kit and purified using AMPure XP (Beckman Coulter). All amplicons were mixed and subjected to an Illumina MiSeq run (paired-end 300; Macrogen). Sequencing data were analyzed according to previous studies (Iida et al., 2020; Suzuki et al., 2018).

Conventional and quantitative RT-PCR analysis

For conventional RT-PCR (Fig. S1), three forelimb blastema, six limb buds and three tails at st40 were used for sampling of mRNA. For quantitative RT-PCR (Fig. 5B), *a-1* crispants and uninjected wild-type embryos at st38 were

used. Four mixtures were analyzed for each genotype (*a-1* and wild type). Each mixture contained six forelimb buds from three animals. In both RT-PCR analyses, RNA was extracted using the ReliaPrep RNA Tissue Miniprep System (Promega) and cDNA was synthesized using a PrimeScript II First Strand cDNA Synthesis Kit (Takara Bio). Other methods were performed as described in a previous study (Toyoda et al., 2003). *Gapdh* was used as the endogenous control. Primers are shown in Table S7.

Limb amputation and bone staining

Limb amputation and bone staining were performed as described previously (Koriyama et al., 2018). The forelimbs were amputated at the most proximal region in the stylopod. The developed and regenerated limbs were fixed in 10% formalin solution at 4°C for at least 2 days and stained with Alizarin Red and Alcian Blue.

Observation of developing and regenerating limbs

The developing and regenerating limbs were observed with a stereoscopic microscope (Leica, MZFL III), and images, including limbs before and after bone staining, were acquired with a microscopy camera (Nikon, DS-Ri2).

Histology

For *in situ* hybridization, fragments for probes were amplified by PCR using cDNA generated from *P. waltl* embryos (st27). Primers are listed in Table S7. The gene coding sequences for *P. waltl* were obtained from iNewt (Matsunami et al., 2019) (http://www.nibb.ac.jp/imori/main/). Each fragment was cloned using the pGEM-T easy vector system (A1360, Promega). Digoxygenin-labeled RNA probes were synthesized by T7 or SP6 RNA polymerase (Roche). WISH for amphibians was performed as described previously (Purushothaman et al., 2019), except for bleaching (6% H_2O_2, 4°C overnight) and permeabilization with 20 µg/ml Proteinase K (FUJIFILM Wako Chemicals) at room temperature for 30 min (FUJIFILM Wako Chemicals). Section *in situ* hybridization was performed as described previously (Kragl et al., 2013) with the following modifications. Before hybridization, sections were permeabilized with 1 µg/ml proteinase K at 37°C for 15 min, and alkaline phosphatase activity was visualized by NBT/BCIP. For serial frozen sections, samples after fixation with MEMFA (0.1 M MOPS pH 7.4, 2 mM EGTA, 1 mM $MgSO_4{\cdot}7H_2O$ and 3.7% formaldehyde) were treated with 30% sucrose/PBS, embedded in OCT compound (Sakura Finetek Japan), and were serially sectioned at 20-µm thickness.

Statistical analysis

Experimental data were analyzed using Welch's two-sample *t*-test and Fisher's exact test. Values of $P<0.05$ were considered statistically significant.

Acknowledgements

The authors wish to thank Dr Hitoshi Yokoyama (Hirosaki University, Hirosaki, Japan) for critical reading of the article and the kind gift of the *hsp70:gene-P2A-EGFP*/I-SceI vector, and Ms Akiko Adachi and Messrs Hiroshi Onishi and Yuuki Senoue (Tottori University, Yonago, Japan) for their technical assistance and newt raising.

Competing interests

The authors declare no competing or financial interests.

Author contributions

Conceptualization: T.T., H.M.; Methodology: T.T., H.M., T.H.; Software: K.T.S.; Validation: T.T., H.M.; Formal analysis: T.T., H.M.; Investigation: T.T., H.M., F.M., Y.S., S.T., T.M., K.M., K.T.S., T.H.; Resources: T.T., H.M., S.S., T.I., K.A., T.H.; Writing - original draft: T.T., H.M., K.T.; Writing - review & editing: T.T., H.M., Y.S., K.T.S., S.S., K.T., K.A.; Visualization: T.T., H.M.; Supervision: T.T.; Project administration: T.T.; Funding acquisition: T.T., H.M., K.T.S., T.H.

Funding

This work was supported by the National Institute for Basic Biology Collaborative Research Program (18–204 to T.H.). This work was partially supported by Japan Society for the Promotion of Science KAKENHI grants (26650082, 16H04794 and 20K06656 to T.T., 21K15145 to H.M., 18K06257 to K.T.S. and 16K08467 to T.H.).

Peer review history

The peer review history is available online at https://journals.biologists.com/dev/article-lookup/doi/10.1242/dev.200282.

References

Bastida, M. F., Pérez-Gómez, R., Trofka, A., Zhu, J., Rada-Iglesias, A., Sheth, R., Stadler, H. S., Mackem, S. and Ros, M. A. (2020). The formation of the thumb requires direct modulation of Gli3 transcription by Hoxa13. *Proc. Natl. Acad. Sci. USA* **117**, 1090-1096. doi:10.1073/pnas.1919470117

Bickelmann, C., Frota-Lima, G. N., Triepel, S. K., Kawaguchi, A., Schneider, I. and Fröbisch, N. B. (2018). Noncanonical Hox, Etv4, and Gli3 gene activities give insight into unique limb patterning in salamanders. *J. Exp. Zool. B Mol. Dev. Evol.* **330**, 138-147. doi:10.1002/jez.b.22798

Capellini, T. D., Di Giacomo, G., Salsi, V., Brendolan, A., Ferretti, E., Srivastava, D., Zappavigna, V. and Selleri, L. (2006). Pbx1/Pbx2 requirement for distal limb patterning is mediated by the hierarchical control of Hox gene spatial distribution and Shh expression. *Development* **133**, 2263-2273. doi:10.1242/dev.02395

Coates, M. I. (1994). The origin of vertebrate limbs. *Development* 1994 Supplement 169-180.

Davis, A. P., Witte, D. P., Hsieh-Li, H. M., Potter, S. S. and Capecchi, M. R. (1995). Absence of radius and ulna in mice lacking hoxa-11 and hoxd-11. *Nature* **375**, 791-795. doi:10.1038/375791a0

Dollé, P., Dierich, A., LeMeur, M., Schimmang, T., Schuhbaur, B., Chambon, P. and Duboule, D. (1993). Disruption of the Hoxd-13 gene induces localized heterochrony leading to mice with neotenic limbs. *Cell* **75**, 431-441. doi:10.1016/0092-8674(93)90378-4

Flowers, G. P., Timberlake, A. T., McLean, K. C., Monaghan, J. R. and Crews, C. M. (2014). Highly efficient targeted mutagenesis in axolotl using Cas9 RNA-guided nuclease. *Development* **141**, 2165-2171. doi:10.1242/dev.105072

Fromental-Ramain, C., Warot, X., Lakkaraju, S., Favier, B., Haack, H., Birling, C., Dierich, A., Doll e, P. and Chambon, P. (1996a). Specific and redundant functions of the paralogous Hoxa-9 and Hoxd-9 genes in forelimb and axial skeleton patterning. *Development* **122**, 461-472. doi:10.1242/dev.122.2.461

Fromental-Ramain, C., Warot, X., Messadecq, N., LeMeur, M., Dollé, P. and Chambon, P. (1996b). Hoxa-13 and Hoxd-13 play a crucial role in the patterning of the limb autopod. *Development* **122**, 2997-3011. doi:10.1242/dev.122.10.2997

Galli, A., Robay, D., Osterwalder, M., Bao, X., Bénazet, J. D., Tariq, M., Paro, R., Mackem, S. and Zeller, R. (2010). Distinct roles of Hand2 in initiating polarity and posterior Shh expression during the onset of mouse limb bud development. *PLoS Genet.* **6**, e1000901. doi:10.1371/journal.pgen.1000901

Gardiner, D. M., Blumberg, B., Komine, Y. and Bryant, S. V. (1995). Regulation of HoxA expression in developing and regenerating axolotl limbs. *Development* **121**, 1731-1741. doi:10.1242/dev.121.6.1731

Hayashi, T., Yokotani, N., Tane, S., Matsumoto, A., Myouga, A., Okamoto, M. and Takeuchi, T. (2013). Molecular genetic system for regenerative studies using newts. *Dev. Growth Differ.* **55**, 229-236. doi:10.1111/dgd.12019

Hayashi, S., Kobayashi, T., Yano, T., Kamiyama, N., Egawa, S., Seki, R., Takizawa, K., Okabe, M., Yokoyama, H. and Tamura, K. (2015). Evidence for an amphibian sixth digit. *Zool. Lett.* **1**, 17. doi:10.1186/s40851-015-0019-y

Hayashi, T., Nakajima, M., Kyakuno, M., Doi, K., Manabe, I., Azuma, S. and Takeuchi, T. (2019). Advanced microinjection protocol for gene manipulation using the model newt Pleurodeles waltl. *Int. J. Dev. Biol.* **63**, 281-286. doi:10.1387/ijdb.180297th

Iida, M., Suzuki, M., Sakane, Y., Nishide, H., Uchiyama, I., Yamamoto, T., Suzuki, K. T. and Fujii, S. (2020). A simple and practical workflow for genotyping of CRISPR-Cas9-based knockout phenotypes using multiplexed amplicon sequencing. *Genes Cells* **25**, 498-509. doi:10.1111/gtc.12775

Kmita, M., Tarchini, B., Zàkàny, J., Logan, M., Tabin, C. J. and Duboule, D. (2005). Early developmental arrest of mammalian limbs lacking HoxA/HoxD gene function. *Nature* **435**, 1113-1116. doi:10.1038/nature03648

Koriyama, K., Sakagami, R., Myouga, A., Hayashi, T. and Takeuchi, T. (2018). Newts can normalize duplicated proximal-distal disorder during limb regeneration. *Dev. Dyn.* **247**, 1276-1285. doi:10.1002/dvdy.24685

Kragl, M., Roensch, K., Nüsslein, I., Tazaki, A., Taniguchi, Y., Tarui, H., Hayashi, T., Agata, K. and Tanaka, E. M. (2013). Muscle and connective tissue progenitor populations show distinct Twist1 and Twist3 expression profiles during axolotl limb regeneration. *Dev. Biol.* **373**, 196-204. doi:10.1016/j.ydbio.2012.10.019

Lappin, T. R., Grier, D. G., Thompson, A. and Halliday, H. L. (2006). HOX genes: seductive science, mysterious mechanisms. *Ulster Med. J.* **75**, 23-31.

Leite-Castro, J., Beviano, V., Rodrigues, P. N. and Freitas, R. (2016). HoxA Genes and the fin-to-limb transition in vertebrates. *J. Dev. Biol.* **4**, 10. doi:10.3390/jdb4010010

Maden, M. (1977). The regeneration of positional information in the amphibian limb. *J. Theor. Biol.* **69**, 735-753. doi:10.1016/0022-5193(77)90379-4

Makanae, A. and Satoh, A. (2018). Ectopic Fgf signaling induces the intercalary response in developing chicken limb buds. *Zool. Lett.* **4**, 8. doi:10.1186/s40851-018-0090-2

Matsunami, M., Suzuki, M., Haramoto, Y., Fukui, A., Inoue, T., Yamaguchi, K., Uchiyama, I., Mori, K., Tashiro, K., Ito, Y. et al. (2019). A comprehensive reference transcriptome resource for the Iberian ribbed newt Pleurodeles waltl, an emerging model for developmental and regeneration biology. *DNA Res.* **26**, 217-229. doi:10.1093/dnares/dsz003

McCusker, C., Bryant, S. V. and Gardiner, D. M. (2015). The axolotl limb blastema: cellular and molecular mechanisms driving blastema formation and limb regeneration in tetrapods. *Regeneration (Oxf)* **2**, 54-71. doi:10.1002/reg2.32

Meyer, A., Schloissnig, S., Franchini, P., Du, K., Woltering, J. M., Irisarri, I., Wong, W. Y., Nowoshilow, S., Kneitz, S., Kawaguchi, A. et al. (2021). Giant lungfish genome elucidates the conquest of land by vertebrates. *Nature* **590**, 284-289. doi:10.1038/s41586-021-03198-8

Nacu, E. and Tanaka, E. M. (2011). Limb regeneration: a new development? *Annu. Rev. Cell Dev. Biol.* **27**, 409-440. doi:10.1146/annurev-cellbio-092910-154115

Nakamura, T., Gehrke, A. R., Lemberg, J., Szymaszek, J. and Shubin, N. H. (2016). Digits and fin rays share common developmental histories. *Nature* **537**, 225-228. doi:10.1038/nature19322

Naito, Y., Hino, K., Bono, H. and Ui-Tei, K. (2015). CRISPRdirect: software for designing CRISPR/Cas guide RNA with reduced off-target sites. *Bioinformatics* **31**, 1120-1123. doi:10.1093/bioinformatics/btu743

Paço, A. and Freitas, R. (2018). Hox D genes and the fin-to-limb transition: Insights from fish studies. *Genesis* **56**, e23069. doi:10.1002/dvg.23069

Purushothaman, S., Elewa, A. and Seifert, A. W. (2019). Fgf-signaling is compartmentalized within the mesenchyme and controls proliferation during salamander limb development. *Elife* **8**, e48507. doi:10.7554/eLife.48507

Roensch, K., Tazaki, A., Chara, O. and Tanaka, E. M. (2013). Progressive specification rather than intercalation of segments during limb regeneration. *Science* **342**, 1375-1379. doi:10.1126/science.1241796

Sakane, Y., Iida, M., Hasebe, T., Fujii, S., Buchholz, D. R., Ishizuya-Oka, A., Yamamoto, T. and Suzuki, K. T. (2018). Functional analysis of thyroid hormone receptor beta in Xenopus tropicalis founders using CRISPR-Cas. *Biol. Open* **7**, bio030338. doi:10.1242/bio.030338

Satoh, A., Endo, T., Abe, M., Yakushiji, N., Ohgo, S., Tamura, K. and Ide, H. (2006). Characterization of Xenopus digits and regenerated limbs of the froglet. *Dev. Dyn.* **235**, 3316-3326. doi:10.1002/dvdy.20985

Schneider, I. and Shubin, N. H. (2013). The origin of the tetrapod limb: from expeditions to enhancers. *Trends Genet.* **29**, 419-426. doi:10.1016/j.tig.2013.01.012

Sheth, R., Bastida, M. F., Kmita, M. and Ros, M. (2014). "Self-regulation," a new facet of Hox genes' function. *Dev. Dyn.* **243**, 182-191. doi:10.1002/dvdy.24019

Shi, D. L. and Boucaut, J. C. (1995). The chronological development of the urodele amphibian Pleurodeles waltl (Michah). *Int. J. Dev. Biol.* **39**, 427-441.

Stocum, D. L. (2017). Mechanisms of urodele limb regeneration. *Regeneration (Oxf)* **4**, 159-200. doi:10.1002/reg2.92

Suzuki, M., Hayashi, T., Inoue, T., Agata, K., Hirayama, M., Shigenobu, S., Takeuchi, T., Yamamoto, T. and Suzuki, K. T. (2018). Cas9 ribonucleoprotein complex allows direct and rapid analysis of coding and noncoding regions of target genes in Pleurodeles waltl development and regeneration. *Dev. Biol.* **443**, 127-136. doi:10.1016/j.ydbio.2018.09.008

Tanaka, M. (2016). Fins into limbs: Autopod acquisition and anterior elements reduction by modifying gene networks involving 5'Hox, Gli3, and Shh. *Dev. Biol.* **413**, 1-7. doi:10.1016/j.ydbio.2016.03.007

Torok, M. A., Gardiner, D. M., Shubin, N. H. and Bryant, S. V. (1998). Expression of HoxD genes in developing and regenerating axolotl limbs. *Dev. Biol.* **200**, 225-233. doi:10.1006/dbio.1998.8956

Toyoda, M., Shirato, H., Nakajima, K., Kojima, M., Takahashi, M., Kubota, M., Suzuki-Migishima, R., Motegi, Y., Yokoyama, M. and Takeuchi, T. (2003). jumonji downregulates cardiac cell proliferation by repressing cyclin D1 expression. *Dev. Cell* **5**, 85-97. doi:10.1016/S1534-5807(03)00189-8

Wagner, G. P., Khan, P. A., Blanco, M. J., Misof, B. and Liversage, R. A. (1999). Evolution of Hoxa-11 expression in amphibians: is the urodele autopodium an innovation? *Integr. Comp. Biol.* **39**, 686-694. doi:10.1093/icb/39.3.686

Wellik, D. M. and Capecchi, M. R. (2003). Hox10 and Hox11 genes are required to globally pattern the mammalian skeleton. *Science* **301**, 363-367. doi:10.1126/science.1085672

Woltering, J. M. and Duboule, D. (2010). The origin of digits: expression patterns versus regulatory mechanisms. *Dev. Cell* **18**, 526-532. doi:10.1016/j.devcel.2010.04.002

Woltering, J. M., Holzem, M. and Meyer, A. (2019). Lissamphibian limbs and the origins of tetrapod hox domains. *Dev. Biol.* **456**, 138-144. doi:10.1016/j.ydbio.2019.08.014

Yokouchi, Y., Sasaki, H. and Kuroiwa, A. (1991). Homeobox gene expression correlated with the bifurcation process of limb cartilage development. *Nature* **353**, 443-445. doi:10.1038/353443a0

Zákány, J. and Duboule, D. (2007). The role of Hox genes during vertebrate limb development. *Curr. Opin. Genet. Dev.* **17**, 359-366. doi:10.1016/j.gde.2007.05.011

Zákány, J., Fromental-Ramain, C., Warot, X. and Duboule, D. (1997). Regulation of number and size of digits by posterior Hox genes: a dose-dependent mechanism with potential evolutionary implications. *Proc. Natl. Acad. Sci. USA* **94**, 13695-13700. doi:10.1073/pnas.94.25.13695

Zákány, J., Kmita, M. and Duboule, D. (2004). A dual role for Hox genes in limb anterior-posterior asymmetry. *Science* **304**, 1669-1672. doi:10.1126/science.1096049

Zhang, Y., Larsen, C. A., Stadler, H. S. and Ames, J. B. (2011). Structural basis for sequence specific DNA binding and protein dimerization of HOXA13. *PLoS One* **6**, e23069. doi:10.1371/journal.pone.0023069